Middle East coastal ecosystem response to middle-to-late Holocene abrupt climate changes

D. Kaniewski*†‡, E. Paulissen§, E. Van Campo*, M. Al-Maqdissi¶, J. Bretschneider‖, and K. Van Lerberghe‖

*ECOLAB - Laboratoire d'Ecologie Fonctionnelle, Université Paul Sabatier-Toulouse 3, Unité Mixte de Recherche 5245 Centre National de la Recherche Scientifique, Institut National Polytechnique de Toulouse, 29 Rue Jeanne Marvig, 31055 Toulouse, France; †Center for Archaeological Sciences and §Physical and Regional Geography Research Group, Katholieke Universiteit Leuven, Celestijnenlaan 200E, 3001 Heverlee, Belgium; ¶Directorate-General of Antiquities, Damascus, Syria; and ‖Near Eastern Studies Unit, Katholieke Universiteit Leuven, Faculteit Letteren, Blijde-Inkomststraat 21, 3000 Leuven, Belgium

Edited by Ofer Bar-Yosef, Harvard University, Cambridge, MA, and approved July 16, 2008 (received for review April 11, 2008)

The Holocene vegetation history of the northern coastal Arabian Peninsula is of long-standing interest, as this Mediterranean/semiarid/arid region is known to be particularly sensitive to climatic changes. Detailed palynological data from an 800-cm alluvial sequence cored in the Jableh plain in northwest Syria have been used to reconstruct the vegetation dynamics in the coastal lowlands and the nearby Jabal an Nuşayriyah mountains for the period 2150 to 550 B.C. Corresponding with the 4.2 to 3.9 and 3.5 to 2.5 cal kyr BP abrupt climate changes (ACCs), two large-scale shifts to a more arid climate have been recorded. These two ACCs had different impacts on the vegetation assemblages in coastal Syria. The 3.5 to 2.5 cal kyr BP ACC is drier and lasted longer than the 4.2 to 3.9 cal kyr BP ACC, and is characterized by the development of a warm steppe pollen-derived biome (1100–800 B.C.) and a peak of hot desert pollen-derived biome at 900 B.C. The 4.2 to 3.9 cal kyr BP ACC is characterized by a xerophytic woods and shrubs pollen-derived biome *ca.* 2050 B.C. The impact of the 3.5 to 2.5 cal kyr BP ACC on human occupation and cultural development is important along the Syrian coast with the destruction of Ugarit and the collapse of the Ugarit kingdom at *ca.* 1190 to 1185 B.C.

pollen-derived biomes | Tell Tweini | Syria | bond events

The Levantine part of the Arabian Peninsula is extremely rich in archaeological sites, and therefore well suited to study the relationships between natural environment and human societies. High-resolution middle-to-late Holocene terrestrial palaeorecords are still rare in this area. In this article, the impacts of climate forcing and human pressure on past vegetation were evaluated through the reconstruction of ecosystem dynamics in the climatically sensitive zone of coastal Syria (Fig. 1). The study area is located in the Fertile Crescent, at the transition between Mediterranean and subtropical climates. The coastal lowlands are separated from the Ghab depression to the east by the Jabal an Nuşayriyah, a 140-km long north-south mountain range 40- to 50-km wide with peaks >1,200 m above sea level (asl).

Previous studies (1–6) have defined two abrupt climate changes (ACCs) in the Middle East between 3050 and 50 B.C. The first ACC is generally referred as the 4.2 cal kyr BP arid event, covering an estimated time period of 4200 to 3900 cal year BP (2250–1950 B.C.) worldwide (7). During this ACC, a widespread abandonment of the agricultural plains of northern Mesopotamia (2, 8) is noted. It corresponds with the abrupt collapse of the northern provinces of the Akkadian Empire at 4170 ± 150 years BP (9, 10, 11), with the termination of the urban Harrapan civilization in Pakistan (12), the collapse of the Old Kingdom in Egypt (2150 B.C.) (13), and the abandonment of cities and towns in Palestine (14), in western Syria (15), and along the Euphrates (5). The second is the 3.2 cal kyr BP ACC, covering an estimated time period of 3500 to 2500 cal years BP (1550–550 B.C.) worldwide (7). It has drawn less attention despite the collapse of the Ugarit kingdom at *ca.* 1190 to 1185 B.C. (16) and the fall of Hellenistic, Anatolian, and Levantine coastal cities all attributed to the invasions of the so-called "Sea People" (17).

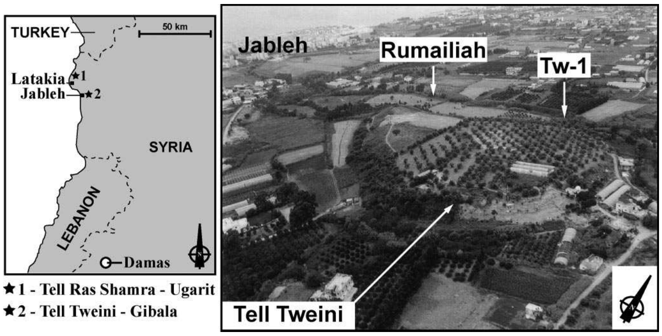

Fig. 1. The northern Arabian Peninsula with the geographical location of Jableh, Tell Tweini-Gibala, and the Rumailiah alluvial plain with core TW-1.

At the end of the late Bronze Age, archaeological evidence shows a massive devastation in western Asia, and most of the cities in Anatolia, Syria, and Palestine were destroyed at *ca.* 1200 B.C. This regional decline was potentially caused by a succession of catastrophic droughts, followed by economic collapse and social chaos (17). A Dead Sea level drop beneath −390 m below sea level (bsl) (3, 4). and increased $\delta^{18}O$ values along the Eastern Mediterranean coast (2, 18) and in the Soreq Cave (1) confirm drier climatic conditions during the same period, strengthening the climate hypothesis. As past ACCs have been put forward as the main driving forces modulating urbanization and human behavior in the ancient Fertile Crescent (4, 5, 9), this article aims to detail the environmental impact of the 3.5 to 2.5 cal kyr BP ACC in the Middle East.

Jableh is a Syrian coastal town (see Fig. 1) located 28-km south of the modern harbor of Latakia and 40-km south of the ancient famous port city of Ugarit in ancient northern Phoenicia (16). The pear-shaped Tell Tweini (35°22′17.93″ N, 35°56′12.60″ E, elevation: 19 to 27 m asl, surface: 11.6 ha), the potential Bronze Age harbor town of Gibala, lies east of Jableh at ≈1.75 km from the seashore. Gibala is mentioned for the first time in an Ugaritic document (Akkadian tablet PRU 4, 71–76) from the second half of the 14th century B.C., when Niqmepa was king in Ugarit (1350–1300 B.C.). This tablet suggests that Gibala belonged to the state of Ugarit (19). Gibala has also been mentioned later in an Assyrian text of Tiglatpileser III (*ca.* 738 B.C.).

Author contributions: D.K. and E.P. designed research; D.K. performed research; D.K., E.P., E.V.C., M.A.-M., J.B., and K.V.L. analyzed data; and D.K., E.P., and E.V.C. wrote the paper.

The authors declare no conflict of interest.

This article is a PNAS Direct Submission.

[‡] To whom correspondence should be addressed. E-mail: kaniewsk@cict.fr.

www.pnas.org/cgi/doi/10.1073/pnas.0803533105

An 800-cm detailed pollen record from the alluvial deposits of the Rumailiah river, just north of Gibala-Tell Tweini (see Fig. 1), supported by a chronology based on four AMS ^{14}C age determinations on charred plant macroremains, was used to decipher the specific environmental conditions prevailing in northwest Syria during the middle-to-late Holocene. Pollen data have been converted to plant functional types (PFTs) and to pollen-derived biomes (PdBs) (20, 21) with the aim to evaluate the impact of these consecutive ACCs on ancient coastal ecosystems and to detail the 3.5 to 2.5 cal kyr BP dry event.

Climate. The Syrian coastal lowland enjoys a typical Mediterranean climate with cool, wet winters and hot, dry summers. The mean annual temperature and precipitation recorded at Latakia (35.5 N, 35.8 E, 7 m asl, 1960–1990) are 19.5°C and 811.4 mm. The cumulated rainfall amounts from June to September are <17 mm. During winter, precipitation mainly originates from eastward propagating, midlatitude cyclones generated in the North Atlantic and in the eastern Mediterranean Sea. The north-south orientated Jabal an Nuşayriyah mountain range affects the precipitation amounts positively in the coastal area and negatively inland. During the summer, the area is influenced by the subtropical high-pressure system, which almost completely inhibits rainfall.

Results and Discussion

Numerical Analyses. Principal components analysis (PCA) ordination was selected because it is a nonparametric method of extracting relevant information from complex datasets (Fig. 2). Most of the variance is accounted for the first PCA-Axis, with 68.38% of total inertia. PCA-Axes 2 and 3 account for 18.04% and 7.53% of total inertia, respectively. PCA-Axis 1 loadings distribute the PdBs classified as steppe-desert with hot desert (HODE) (0.6181) and warm steppe (WAST) (0.1832) in positive values. The negative values correspond to the PdBs classified as woods-forest with warm mixed forest (WAMX) (−0.6512) and xerophytic woods/shrubs (XERO) (−0.1219). Linear detrended cross-correlations were applied to distinguish the positive or negative PdB-responses with selective incidences. Human-induced changes of PdBs classified as woods-forest to PdBs classified as steppe-desert (Fig. 3) may be reflected by a significant correlation coefficient at lag 0 ($P = 0.05$) and positive lags in cross-correlation results between the primary anthropogenic indicators and the PdBs classified as steppe-desert (± 8 samples, ± 200 calibrated year window). No positive correlation was observed between both variables in the time-window, suggesting no direct relationships between human pressure and the introduction of a WAST landscape in the Syrian coastal area.

The PCA-Axis 1 ordination of the TW-1 data (see Fig. 2) therefore relates different vegetation assemblages according to ACC-related variations in moisture availability through time: (*i*) Three major positive deviations on the PCA-Axis 1 indicative of dry periods have been recorded: before *ca.* 2100 B.C., during the time period 1175 to 800 B.C., and from *ca.* 600 B.C. onwards. The 1175 to 800 B.C. dry event does not remain stable: dryness intensity increases through time and an ≈50 year negative deviation suggests a short-term humidity trend. (*ii*) Two main negative deviations of PCA-Axis 1, indicative of wetter periods, have been recorded at *ca.* 1950 to 1175 B.C., with humidity peaks *ca.* 1250 B.C. and *ca.* 800 to 600 B.C.

PdB Diagram. Based on the PdB-scores (see Fig. 2), environmental changes in the Syrian coastal area throughout the 2150 to 550 B.C. period are subdivided into five major time stages. Only the two ACCs are considered.

Stage 1 (4.2–3.9 cal kyr BP ACC). The base of the pollen sequence is situated within the 4.2 to 3.9 cal kyr BP ACC and shows a local semiarid vegetation, with positive PCA-Axis 1 scores and a dominant XERO PdB. Synchronous high WAMX and XERO PdB-scores (see Fig. 2) in stage 1 suggest an integration in the pollen assemblages of the altitudinal gradient of biomes between the coast and the wetter Jabal an Nuşayriyah mountains. During this ACC, the vegetation of coastal Syria appears to be more arid than what is registered on average in the pollen record, a probable ecological response to lower winter precipitation than today. The forest cover (maximum 55% of the total pollen sum) is mainly composed of xerophytic shrubs and thorny scrubs (maximum recorded values: trees, 17%; shrubs, 46% of the total pollen sum) resulting in a shrubby landscape without loss of terrestrial plant diversity. The input of freshwater (IoF) and the increased water availability (Iwa) indices are low, suggesting low water amounts in the Jableh area.

The 4.2 to 3.9 cal kyr BP ACC has been registered worldwide, but is mainly documented at middle and low latitudes (5, 7, 22). In the Middle East and in southern Asia its importance has been stressed in northeast Syria at Tell Leilan, the ancient city of Shekhna (9), and in the Indus Valley (12). The agricultural plains between the Tigris and Euphrates rivers were subjected to an important shift toward aridity at 4170 ± 150 year BP (9, 11), with population migrations toward the south of ancient Mesopotamia. This event, known as the "collapse of the Akkadian empire's northern provinces" (23), is reflected at Tell Leilan by an important accumulation of windblown silts (24). A marine sediment core from the Gulf of Oman (25) documents an abrupt increase in aeolian dust possibly blown in from Mesopotamia at 4025 ± 125 calendar year BP. This ACC is also reflected by an enhanced salinization of the Indus delta and is correlated with the end of the urban Harrapan civilization in Pakistan (12). A pronounced arid event in Lake Awafi (Rub'al-khali desert) is evidenced at 2150 B.C. (8). A dramatic drop of the Dead Sea level (≈45 m) starts at *ca.* 2250 B.C. (3). Lower precipitation amounts in the southern Levant (1), brine sediments from the northern Red Sea (26), $\delta^{13}C$ and $\delta^{18}O$ data from Göbekli Tepe (27) and Lake Zeribar (28), all point toward a shift to more arid conditions in western Asia during the time period *ca.* 2250 to 2050 B.C. Evidence of desertion of urban centers and cities is particularly impressive in Palestine between 2350 and 2000 B.C., whereas northwards many cities were destroyed (29).

In coastal Syria, the history of nearby towns appears to be complex. Gibala-Tell Tweini was inhabited during the end of the third millennium B.C. [early Bronze Age (EBA) IVA–B] as attested by two architectural phases (Tweini XA–XB) (19). At Tell Sianu, 6-km north of Tell Tweini, large urban structures are known from the EBA IVA, whereas the EBA IVB corresponds to an abandonment phase (30). At Ugarit, a hiatus at the end of the EBA is also registered between archaeological levels III and II (16). In the Jableh record, the beginning of this ACC is not dated, but its termination corresponds with the onset of the increase of the WAMX PdB-scores dated at *ca.* 1950 B.C.

Stage 3 (3.5–2.5 cal kyr BP ACC). After ≈800 years of wetter conditions, inferred from the increases in PdB, classified as forest, a new trend to more arid conditions is initiated in the Syrian coastal area by the fall of WAMX PdB-scores and a renewed increase of XERO PdB-scores dated at *ca.* 1175 B.C. (see Fig. 2).

Contemporaneous with this major shift in vegetation assemblages, the Ugarit kingdom collapsed at 1190 to 1185 B.C. (16), the Egyptian presence in the Levant ended *ca.* 1150 to 1135 B.C. (31), Assyria and Babylonia suffered from famine (32), whereas city abandonment, social chaos, and invasions of the Sea People are noted in the Levant (17). In general, the 12th Century BC was a time of crisis in the Mediterranean as many civilizations disappeared and towns were destroyed (33).

The characteristics of the 3.5 to 2.5 cal kyr BP worldwide ACC

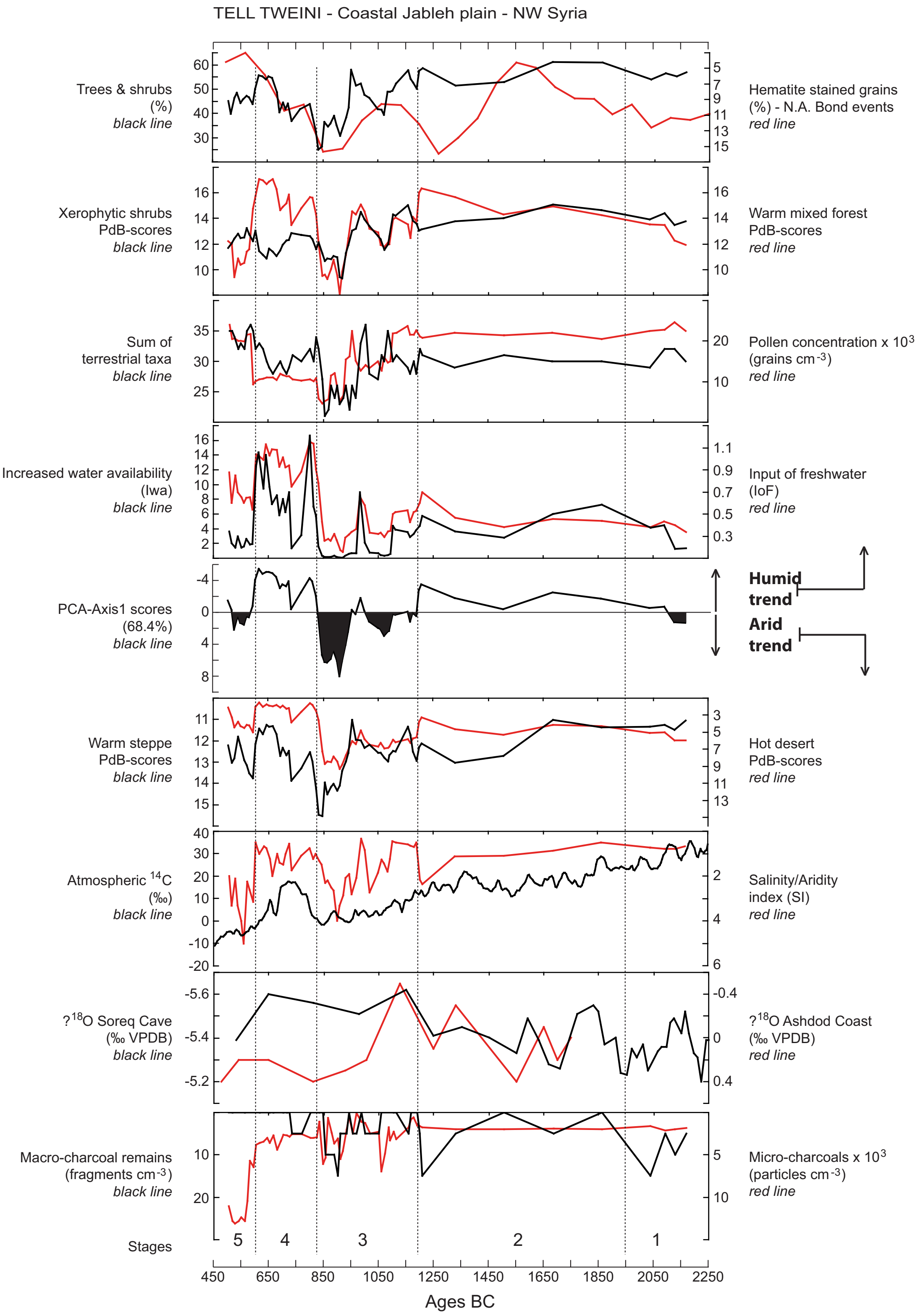

Fig. 2. Tell Tweini: Core TW-1 linear age-scale pollen-derived biomes diagram with salinity/aridity (SI), input of freshwater (IoF) and increased water availability (Iwa) indices. $\delta^{18}O$ data originate from the Soreq Cave (1) and from the Ashdod coast (14). The atmospheric $\delta^{14}C$ curve (32) and North Atlantic Bond events (8) are plotted to match the Jableh plain pollen data with global climatic changes.

are clearly depicted in the evolution of the PCA-Axis 1 scores (see Fig. 2), demonstrating a gradual intensifying pulse-by-pulse response of the vegetation (XERO, WAST, HODE) to increasing drought from 1175 B.C. onwards. The full development of desert conditions is evidenced by the intense final peak of the HODE PdB-score at 900 B.C. The vegetation responds with a dramatic reduction of the forest cover, an opening of the landscape (AP <25% of the total pollen sum), and a loss of

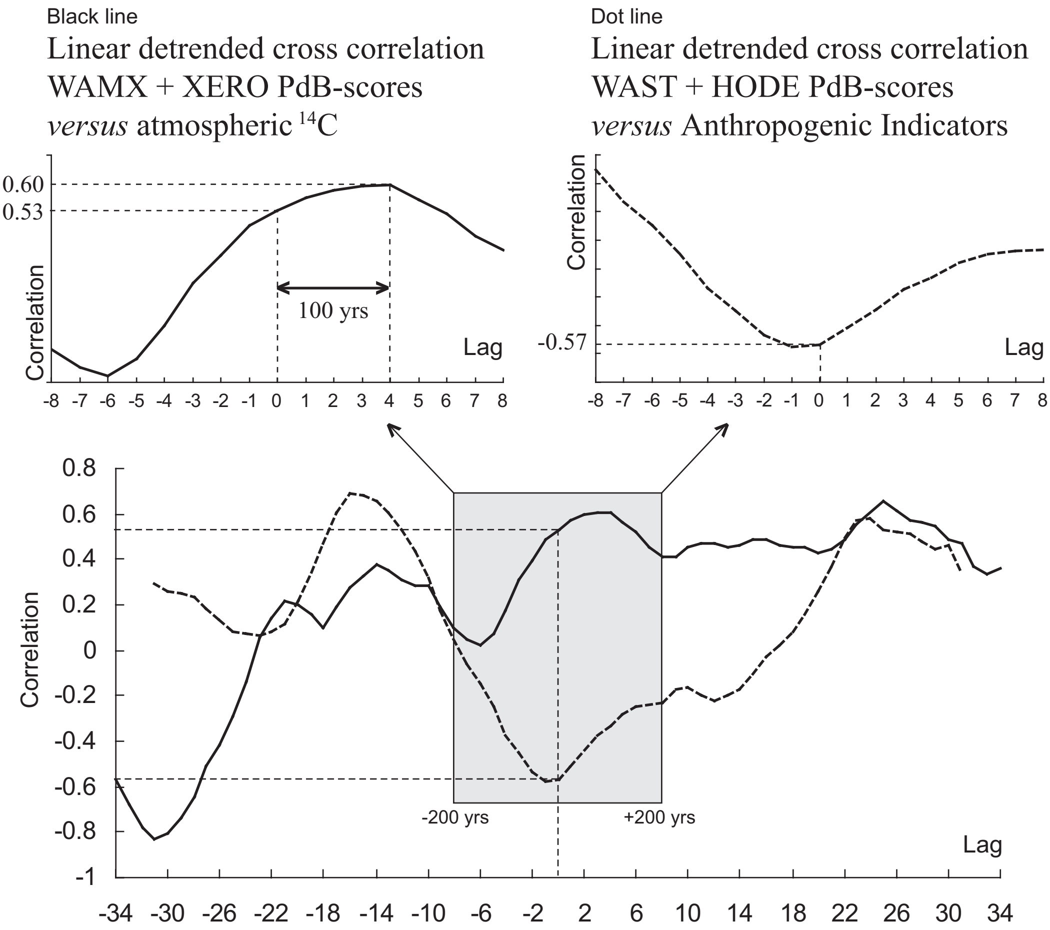

Fig. 3. Cross-correlograms: WAMX + XERO PdB-scores versus atmospheric $\delta^{14}C$ (32) and WAST + HODE PdB-scores versus anthropogenic indicators. Vertical axes show correlation coefficients. Significance level $P = 0.05$.

terrestrial plant diversity. This drought is also evidenced by the salinity/aridity-index (SI), IoF, and Iwa indices.

A small magnitude 50-year shift (*ca.* 1000–950 B.C.) toward wetter conditions within stage 3 is evidenced by a negative deviation in PCA-Axis 1, lower SI, and increased IoF indices. Synchronous increases of the WAMX and XERO PdB-scores suggest higher inputs of freshwater in the coastal area and the Jabal an Nuşayriyah mountains.

A dry and warm climate dated *ca.* 1200 to 900 B.C. has been also suggested for the Middle East (34). A $\delta^{18}O$ study in the southeastern Mediterranean (2, 18) suggests that aridification, reflected by enhanced evaporation rates, started at 1050 B.C., succeeding by a 1650 to 1050 B.C. humid phase. This climatic shift can be correlated with changes in atmospheric moisture over India (35) and low lake levels in Turkey (36). Peaking values of arid/saline Chenopodiaceae and a collapse of agriculture at *ca.* 1050 to 850 B.C. in the Ze'elim and Ein Feshkha pollen sequences (6) also reflect dry conditions. The onset of an aridification is recorded in the Arabian Sea somewhat earlier, at *ca.* 1150 B.C. (37) and much earlier, at *ca.* 1550 B.C. in the Dead Sea, where it is reflected by low lake levels (until −417 m bsl) and a windblown sand layer at the lake bottom (4).

The data related to the 3.5 to 2.5 cal kyr BP global ACC suggest along the Syrian coast a complex shift from an open deciduous forest toward a more arid/saline-tolerant vegetation cover, which starts at *ca.* 1175 B.C. and peaks *ca.* 900 B.C. (2750 ± 40 ^{14}C BP). The collapse of the late Bronze Age urban and political system *ca.* 1200 B.C. is attested in Ugarit and Tell Tweini (Tweini VIIIB) by military action events (Sea People invasions) with large fire destruction (16, 19). The abandonment of Gibala-Tell Tweini has been recorded during part of Iron Age I. Ugarit was not rebuilt during Iron Age I and II, whereas Gibala flourished with large urban structures during Iron I, II and III (Tweini VII–V). Architectural and urban patterns changed drastically between the Iron Age I and II, *ca.* 900 B.C. (19). During this ACC, the nearby coastal cities reacted differently again, as was the case in the previous ACC. This was probably because of local circumstances. Water shortages were eventually less severe or nonexistent at Tell Tweini/Gibala, which is built near abundant springs.

At *ca.* 800 B.C., a strong increase of WAMX PdB-scores, a negative deviation in PCA-Axis 1 scores, the recovery of trees, and the higher IoF values all point to a return of wetter climatic conditions during ≈200 years. This wetter phase is similar to the previous 1450 to 1175 B.C. humid episode. The *ca.* 800 B.C. shift toward humidity marks the end of the global 3.5 to 2.5 cal kyr BP ACC in northwest Syria. In the top of the Jableh sequence, a dry spell is registered with an estimated age of 600 B.C.

Climate. Several causes have been invoked to explain the post-6000 calendar year BP ACCs, among which solar forcing appears to be a plausible one (7, 27, 38). Solar influence on climatically-controlled development of desert-steppe environments in the Jableh plain during the 2150 to 500 B.C. interval was tested by

Table 1. AMS ^{14}C calibrated ages (2σ and 1σ) for core TW-1

Sample	Depth, cm	Laboratory codes	Material	δ^{13}C, ‰ PdB	Conventional ^{14}C age (years BP ± 1σ)	cal (2σ) age range rounded (B.C.)	cal (1σ) age range rounded (B.C.)	Interception with the calibration curve (32)
TWE04 EP35	395	Beta-229047	charcoal	−22.7	2750 ± 40BP	1000–810	920–840	900 B.C.
TWE04 EP57	680	Beta-229048	charcoal	−26.9	2970 ± 40BP	1310–1050	1270–1120	1210 B.C.
TWE04 EP73	755	Beta-229049	charcoal	−27.3	3710 ± 40BP	2200–2000	2150–2030	2060 B.C. and 2080* B.C. and 2130 B.C.
TWE04 EP75	785	Beta-233430	charcoal	−26.3	3680 ± 40BP	2150–1950	2130–2020	2040 BC and 2100* BC and 2110 BC

Asterisks indicate the most probable dates.

a cross-correlation analysis between the δ^{14}C solar proxy and PdBs classified as woods-forest (see Fig. 3). Correlation results show a significant positive correlation ($P = 0.05$) in the time window between increases in atmospheric δ^{14}C values indicative of lower solar irradiance and PdBs classified as woods-forest. These results would confirm the role of solar variability as a driving force of ACCs, although physical mechanisms linking solar and climate changes remain unclear (7, 12). The time-interval covered by the TW-1 pollen sequence is not sufficiently long to derive firm links between solar forcing and vegetation changes, but the Tweini data strongly suggest that solar variability is a main cause behind middle to late Holocene precipitation changes over the Near East.

Droughts in the eastern Mediterranean were also associated with cooling periods in the North Atlantic for the past 55 kyr (39). The impact of the North Atlantic oscillation on the modern Middle Eastern climate has been demonstrated (40), emphasizing the potential role of the North Atlantic variability to explain the Holocene climate changes in the Middle East. The correspondence between the arid stages 1 and 3 at coastal Syria and the Bond events 3 and 2 identified in North Atlantic core MC52-V29–191 by the bimodal increase of ice rafted hematite stained grains (HSG) (38) (see Fig. 2), shows that Holocene cold events in the Atlantic Ocean have different climatic signatures. The dry/wet oscillation of the 1175 to 800 B.C. ACC deduced from biome changes is well correlated with the second peak of HSG (Bond event 2) at 900 B.C., whereas a much weaker correlation is observed for the ≈4.2 to 3.9 cal kyr BP ACC with Bond event 3.

Conclusion

The TW-1 core data demonstrate that for two successive ACCs, climate plays the major role in the composition and distribution of biomes in coastal Syria. During the 4.2 to 3.9 cal kyr BP ACC, PdBs classified as woods-shrubs developed, resulting in shrubby and thorny vegetation types. The potential role of this ACC on the cultural development in the Middle East has been abundantly documented (5, 9, 11, 12, 29). During the 1175 to 800 B.C. ACC, the development of steppe/desert conditions progressively transformed the coastal lowlands into a hot desert biome culminating at 900 B.C. Also during this ACC, human occupation and cultural development changed dramatically. The Tell Tweini pollen sequence has demonstrated that abrupt climatic changes toward aridity as a surrogate for water and food shortages are a fundamental trigger behind social, political, and economic decision-making of ancient societies during the middle-to-late Holocene in the Middle East.

Methods

Core, AMS ^{14}C, and Chronology. An 800-cm continuous core (TW-1: 35°22′22.94′′ N, 35°56′12.49′′ E, 17 m asl) was retrieved from the alluvial deposits of the Rumailiah river, 1.75 km from the coast near Jableh, and analyzed to document the vegetation dynamics from *ca.* 2150 to 550 B.C. in coastal Syria. All deposits were sampled with a ramguts corer (length: 100 cm; Ø: 7.5 cm). AMS ^{14}C age determinations (Table 1), based on charred plant macroremains, were obtained for four levels. All ^{14}C ages are processed after standard pretreatment acid-alkaline-acid, quoted in conventional ^{14}C year corrected by normalizing δ^{13}C values and calibrated by the calibration dataset Calib Rev 5.0.1 (41). The age determinations are expressed in B.C. using the year 1950 as time-reference. The chronology calculated for the upper part of the sequence is confirmed by the presence of Iron Age ceramics at different depths. Two statistically identical AMS dates, situated near the bottom of the sequence (at 785-cm and 755-cm depth, see Table 1), within the 2σ age range 2200 to 1950 B.C. (mean age of the two AMS age determinations: 3695 ± 28 BP, 2σ age ranges 2145–2015 B.C.), suggest a high sedimentation rate during that time. Three samples are situated within the 2σ age range 2145 to 2015 B.C. In the calculations, these samples are tentatively placed at 2130, 2090, and 2040 B.C. The age of the 800-cm sample has been computed at *ca.* 2150 B.C.

Pollen Grains, PFTs, and Pollen-Derived Biomes. A total of 62 samples were prepared for pollen analysis using the standard palynological procedure. Pollen data have been converted into PFTs (20, 21) and a pollen-derived biomization of the PFTs has been elaborated following the detailed published methods (20, 21). The notation used is similar to the regional studies in the Mediterranean and Kazakhstan (21) with WAST, HODE, XERO, and WAMX.

Different indices have been calculated for each sample: (*i*) A semiquantitative IoF index, using the PFTs by dividing (grass + sedge) by (steppe forb/shrub + warm desert forb/shrub + steppe/desert forb/shrub) to evaluate potential increases in soil moisture. (*ii*) A semiquantitative Iwa index, calculated by dividing evergreen-deciduous *Quercus* by steppe markers (Chenopodiaceae + *Ephedra*). This Iwa-index strengthens the IoF-index. (*iii*) An salinity/aridity-index by dividing (Chenopodiaceae + *Ephedra*) by *Artemisia*. (*iv*) The taxon richness of terrestrial pollen and spores provides a measure of terrestrial plant diversity through time. (*v*) The ratios of arboreal and nonarboreal pollen provide an estimate of the relative forest density.

The regional scale fire history is based on the number of charcoal particles on pollen slides (< 150 μm) and that on larger charcoal remains counted from ≈100-g samples.

Numerical Analyses. Principal components analysis was computed to test the ordination of samples and stages by assessing the major changes in the PdB-scores. The PCA-Axis 1 scores have been added in the pollen-derived biomes diagram to determine the main changes according to the linear age-scale.

Linear detrended cross-correlation concerns the time alignment of two time series by means of the correlation coefficient. For the Jableh data, PdBs have been cross-correlated with atmospheric δ^{14}C (41) to find the maximal match in age and the potential delay between two events (± insolation versus ± trees and shrubs). Steppe-desert PdBs have also been cross-correlated with the eastern Mediterranean primary anthropogenic indicators (*Fraxinus ornus* L., *Juglans regia* L., *Olea europaea*, *Vitis vinifera* L., Poaceae cerealia) to make the distinction between a climatic and an anthropogenic impact on the observed processes. An average sample interval of 25 years has been fixed for the whole sequence (2150–500 B.C.) to determine the lag effect between climatic changes, anthropogenic impact, and PdB responses. A total of ± 8 samples, corresponding with a time window of ±200 years, have been selected as time reference.

ACKNOWLEDGMENTS. This research is funded by the Fonds voor Wetenschappelijk Onderzoek, the Onderzoeksfonds Katholieke Universiteit Leuven, and the Interuniversity Attraction Poles Program VI/34, Belgian Science Policy, Belgium.

1. Bar-Matthews M, Ayalon A, Kaufman A, Wasserburg GJ (1999) The eastern Mediterranean palaeoclimate as a reflection of regional events: Soreq Cave, Israel. *Earth Planet Sci Lett* 166:85–95.
2. Schilman B, Bar-Matthews M, Almogi-Labin A, Luz B (2001) Global climate instability reflected by Eastern Mediterranean marine records during the Late Holocene. *Palaeogeogr Palaeoclimatol Palaeoecol* 176:157–176.
3. Enzel Y, *et al.* (2003) Late Holocene climates of the Near East deduced from Dead Sea level variations and modern regional winter rainfall. *Quaternary Res* 60:263–273.
4. Migowski C, Stein M, Prasad S, Negendank JFW, Agnon A (2006) Holocene climate variability and cultural evolution in the Near East from the Dead Sea sedimentary record. *Quaternary Res* 66:421–431.
5. Staubwasser M, Weiss H (2006) Holocene climate and cultural evolution in the late prehistoric-early historic West Asia. *Quaternary Res* 66:372–387.
6. Neumann FH, Kagan EJ, Schwab MJ, Stein M (2007) Palynology, sedimentology and palaeoecology of the late Holocene Dead Sea. *Quaternary Sci Rev* 26:1476–1498.
7. Mayewski PA, *et al.* (2004) Holocene climate variability. *Quaternary Res* 62:243–255.
8. Parker AG, *et al.* (2004) Holocene vegetation dynamics in the northeastern Rub'al-Khali desert, Arabian Peninsula: A phytolith, pollen and carbon isotope study. *J Quaternary Sci* 19:665–676.
9. Weiss H, *et al.* (1993) The genesis and collapse of third millennium North Mesopotamian civilization. *Science* 261:995–1004.
10. Weiss H (2000) Beyond the Younger Dryas. *Environmental Disaster and the Archaeology of Human Response*, eds Bawden G, Reycraft RM (Maxwell Museum of Anthropology, Albuquerque), pp 75–98.
11. Weiss H, Bradley RS (2001) What drives societal collapse? *Science* 291:609–610.
12. Staubwasser M, Sirocko F, Grootes PM, Segl M (2003) Climate change at the 4.2 ka BP termination of the Indus Valley civilization and Holocene south Asian monsoon variability. *Geophys Res Lett* 30:71–74.
13. Stanley JD, Krom MD, Cliff RA, Woodward JC (2003) Nile flow failure at the end of the Old Kingdom, Egypt: Strontium isotopic and petrologic evidence. *Geoarchaeology* 18:395–402.
14. Dever W (1995) Social structure in the Early Bronze Age IV period in Palestine. In *The Archaeology of Society in the Holy Land*, eds Levy T (Facts on File, New York), pp 282–296.
15. Schwartz G, *et al.* (2000) Excavation and survey in the Jabbul plain. *American J Archaeol* 104:419–462.
16. Yon M (2006) *The City of Ugarit at Tell Ras Shamra.* (Eisenbrauns, Indiana).
17. Weiss B (1982) The decline of the Late Bronze Age civilization as a possible response to climate change. *Climatic Change* 4:173–198.
18. Schilman B, Ayalon A, Bar-Matthews M, Kagan EJ, Almogi-Labin A (2002) Sea-land palaeoclimate correlation in the Eastern Mediterranean region during the late Holocene. *Israel J Earth Sci* 51:181–190.
19. Bretschneider J, Van Lerberghe K (2008) Tell Tweini, ancient Gibala, between 2600 BCE and 333 BCE. *In Search of Gibala, an Archaeological and Historical Study Based on Eight Seasons of Excavations at Tell Tweini (1999–2007) in the A and C Fields*, eds Bretschneider J, Van Lerberghe K (Aula Orientalis, Barcelona), pp 12–66.
20. Prentice IC, Guiot J, Huntley B, Jolly D, Cheddadi R (1996) Reconstructing biomes from palaeoecological data: A general method and its application to European pollen data at 0 and 6 ka. *Climate Dynam* 12:185–194.
21. Tarasov PE, *et al.* (1998) A method to determine warm and cool steppe biomes from pollen data; application to the Mediterranean and Kazakhstan regions. *J Quaternary Sci* 13:335–344.
22. Dalfes HN, Kukla G, Weiss H (1997) *Third Millennium BC Climate Change and Old World Collapse.* (Ed Springer, Berlin–NATO ASI series).
23. deMenocal PB (2001) Cultural responses to climatic change during the late Holocene. *Science* 292:667–673.
24. Kerr RA (1998) Sea-floor dust shows drought felled Akkadian Empire. *Science* 279:325–326.
25. Cullen HM, *et al.* (2000) Climate change and the collapse of the Akkadian empire: Evidence from the deep sea. *Geology* 28:379–382.
26. Arz HW, Lamy F, Pätzold J (2006) A pronounced dry event recorded around 4.2 ka in brine sediments from the northern Red Sea. *Quaternary Res* 66:432–441.
27. Pustovoytov K, Schmidt K, Taubald H (2007) Evidence for Holocene environmental changes in the northern Fertile Crescent provided by pedogenic carbonate coatings. *Quaternary Res* 67:315–327.
28. Stevens LR, Ito E, Schwalb A, Wright Jr HE (2006) Timing of atmospheric precipitation in the Zagros Mountains inferred from a multi-proxy record from Lake Mirabad, Iran. *Quaternary Res* 66:494–500.
29. Issar AS, Zohar M (2004) *Climate Change—Environment and Civilization in the Middle East.* (Ed Springer, Berlin).
30. Al-Maqdissi M (2006) Notes d'Archéologie Levantine VIII. Stratigraphie du Chantier B de Tell Sianu (plaine de Jablé). *Syria* 83:229–246.
31. Bruins HJ, van der Plicht J, Mazar A (2003) ^{14}C dates from Tel Rehov: Iron-Age chronology, pharaohs, and Hebrew kings. *Science* 300:315–318.
32. Alpert P, Neumann J (1989) An ancient correlation between streamflow and distant rainfall in the Near East. *J Near Eastern Studies* 48:313–314.
33. Ward WA, Sharp Joukowsky M (1992) *The Crisis Years: The 12th Century B.C. from beyond the Danube to the Tigris.* (Ed Kendall/Hunt Publ, Dubuque).
34. Neumann J, Perpola S (1987) Climatic change and the eleventh-tenth-century eclipse of Assyria and Babylonia. *J Near Eastern Studies* 46:161–182.
35. Singh G, Wasson RJ, Agrawal DP (1990) Vegetational and seasonal climatic changes since the last full glacial in the Thar Desert, northwestern India. *Rev Palaeobot Palynol* 64:351–358.
36. Lemcke G, Sturm M (1996) ^{18}O and trace elements measurements as proxy for reconstruction of climate change at Lake Van (Turkey). *Third Millenium BC: Climate change and old world collapse*, eds Dalfes HN, Kukla GH, Weiss H (Springer, Berlin), pp 653–678.
37. Lückge A, Doose-Rolinski H, Khan AA, Schulz H, von Rad U (2001) Monsoonal variability in the northeastern Arabian Sea during the past 5000 yr: Geochemical evidence from laminated sediments. *Palaeogeogr Palaeoclimatol Palaeoecol* 167:273–286.
38. Bond G, *et al.* (2001) Persistent solar influence on North Atlantic climate during the Holocene. *Science* 294:2130–2136.
39. Bartov Y, Goldstein SL, Stein M, Enzel Y (2003) Catastrophic arid episodes in the Eastern Mediterranean linked with the North Atlantic Heinrich events. *Geology* 31:439–442.
40. Cullen HM, Kaplan A, Arkin PA, deMenocal PB (2002) Impact of the North Atlantic Oscillation on Middle Eastern climate and streamflow. *Climate Change* 55:315–338.
41. Reimer PJ, *et al.* (2004) IntCal04 Terrestrial radiocarbon age calibration, 26–0 ka BP. *Radiocarbon* 46:1029–1058.